PHYSICAL REVIEW D **84,** 063505 (2011)

What galaxy surveys really measure

Camille Bonvin[*]

Kavli Institute for Cosmology Cambridge and Institute of Astronomy, Madingley Road, Cambridge CB3 OHA, United Kingdom and DAMTP, Centre for Mathematical Sciences, Wilberforce Road, Cambridge CB3 OWA, United Kingdom

Ruth Durrer[†]

Département de Physique Théorique and Center for Astroparticle Physics, Université de Genève, 24 quai Ernest Ansermet, CH-1211 Genève 4, Switzerland and CEA, SPhT, URA 2306, F-91191 Gif-sur-Yvette, France

(Received 26 May 2011; published 2 September 2011)

In this paper we compute the quantity which is truly measured in a large galaxy survey. We take into account the effects coming from the fact that we actually observe galaxy redshifts and sky positions and not true spatial positions. Our calculations are done within linear perturbation theory for both the metric and the source velocities but they can be used for nonlinear matter power spectra. We shall see that the complications due to the fact that we only observe on our background light cone, and that we do not truly know the distance of the observed galaxy but only its redshift, not only cause an additional difficulty, but provide even more a new opportunity for future galaxy surveys.

DOI: 10.1103/PhysRevD.84.063505 PACS numbers: 98.80.−k, 98.62.Py, 98.65.−r

I. INTRODUCTION

All the photons which we receive have been emitted on our past light cone. In cosmology, looking far away always also means looking into the past. If the redshift of the objects under consideration is small, $z \ll 1$, and evolution is relevant only on cosmological time scales, this effect is small and may be neglected. However, for redshifts of order unity or larger, the fact that we are not observing a spatial hypersurface but a part of the background light cone becomes relevant.

If we observe the large scale distribution of galaxies, we usually compare the true, observed distribution with the one of an unperturbed universe with background density $\bar{\rho}$ and measure its fluctuations, $\delta(\mathbf{x}) = (\rho(\mathbf{x}) - \bar{\rho})/\bar{\rho}$, where $\bar{\rho}$ is usually the mean observed galaxy density. This is then cast in the power spectrum,

$$\langle \delta(\mathbf{k})\delta(\mathbf{k}')\rangle = (2\pi)^3\delta(\mathbf{k} - \mathbf{k}')P_\delta(k),$$

where $\delta(\mathbf{k})$ is the Fourier transform of $\delta(\mathbf{x})$ and we assume statistical homogeneity and isotropy. For small galaxy catalogs one may assume that we measure the density fluctuation today, $\delta(\mathbf{x}) = \delta(\mathbf{x}, t_0)$, but already for the Sloan Digital Sky Survey which determines the galaxy distribution out to $z \sim 0.2$ or 0.5 (for luminous red galaxies, LRG's) it is no longer a good approximation, to compare the observed power spectrum with the above defined $P_\delta(t_0)$. Time evolution of P_δ can be taken into account by multiplying the power spectrum with a growth factor. In addition to this, there is the issue of gauge. The density fluctuation $\delta(\mathbf{x}, t)$ which we calculate in a given Friedmann background is not gauge invariant. It depends on the background Friedmann universe that we compare the observed $\rho(\mathbf{x}, t)$ with. This is the cosmological gauge problem [1].

There are several attempts in the literature to deal with these issues, but they are so far incomplete. People have considered individual observational effects like redshift-space distortions [2], the Alcock-Pacinski effect [3], or lensing. A first full treatment is attempted in [4]. In the present paper we shall go beyond this work and determine the spectrum truly in terms of directly observable quantities. We derive gauge-invariant expressions which are correct to first order in perturbation theory and which are straightforward to compare with observations. This is an important first step for this problem, as the gauge issue is mainly relevant on very large scales, where perturbations are small so that first order perturbation theory is justified.

Our results will be most significant for future galaxy catalogs like BOSS [5], DES [6], Pan-Starrs [7] and, especially, Euclid [8], but also an analysis of SLOAN-7 [9] along the lines outlined here is interesting.

Notation.—We work with a flat Friedmann background and in conformal time t such that

$$ds^2 = a^2(t)(-dt^2 + \delta_{ij}dx^i x^j).$$

A photon geodesic in this background which arrives at position $\mathbf{x}_O$ at time t_O and which has been emitted at affine parameter $\lambda = 0$ at time t_S, moving in direction $\mathbf{n}$, is then given by $(x^\mu(\lambda)) = (\lambda + t_S, \mathbf{x}_O + (\lambda + t_S - t_O)\mathbf{n})$. Here $\lambda = t - t_S = r_S - r$, where r is the comoving distance $r = |\mathbf{x}(\lambda) - \mathbf{x}_O|$, and hence $dr = -d\lambda$. We can of course choose $\mathbf{x}_O = 0$.

[*]cbonvin@ast.cam.ac.uk
[†]ruth.durrer@unige.ch

II. THE MATTER FLUCTUATION SPECTRUM IN REDSHIFT SPACE

In a galaxy redshift survey, the observers measure the number of galaxies in direction $\mathbf{n}$ at redshift z; let us call this $N(\mathbf{n}, z)d\Omega_{\mathbf{n}}dz$. They then average over angles to obtain their redshift distribution, $\langle N\rangle(z)dz$. From this they can build directly the redshift density perturbation [10] i.e. the perturbation variable

$$\delta_z(\mathbf{n}, z) = \frac{\rho(\mathbf{n}, z) - \langle\rho\rangle(z)}{\langle\rho\rangle(z)} = \frac{\frac{N(\mathbf{n},z)}{V(\mathbf{n},z)} - \frac{\langle N\rangle(z)}{V(z)}}{\frac{\langle N\rangle(z)}{V(z)}} = \frac{N(\mathbf{n}, z) - \langle N\rangle(z)}{\langle N\rangle(z)} - \frac{\delta V(\mathbf{n}, z)}{V(z)}. \quad (1)$$

Here $V(\mathbf{n}, z)$ is the physical survey volume density per redshift bin, per solid angle. The volume is also a perturbed quantity since the solid angle of observation as well as the redshift bin are distorted between the source and the observer. Hence $V(\mathbf{n}, z) = V(z) + \delta V(\mathbf{n}, z)$. The truly observed quantity is the perturbation in the number density of galaxies,

$$\frac{N(\mathbf{n}, z) - \langle N\rangle(z)}{\langle N\rangle(z)} = \delta_z(\mathbf{n}, z) + \frac{\delta V(\mathbf{n}, z)}{V(z)} \equiv \Delta(\mathbf{n}, z), \quad (2)$$

which therefore must be gauge invariant. Actually, as we shall see, both $\delta_z(\mathbf{n}, z)$ and $\delta V(\mathbf{n}, z)/V(z)$ are gauge invariant. This is not surprising, as we could measure the volume perturbation also with tracers other than galaxies, and it is therefore measurable by itself and hence gauge invariant.

We neglect biasing in our treatment as we want to keep the expressions as model independent as possible. We shall add only some comments on how simple linear biasing could be included.

A. Computation of $\delta_z(\mathbf{n}, z)$

Let us first relate $\delta_z(\mathbf{n}, z)$ to the well-known gauge dependent quantity $\delta(\mathbf{x}, t)$. For this we note that to first order

$$\delta_z(\mathbf{n}, z) = \frac{\rho(\mathbf{n}, z) - \bar\rho(z)}{\bar\rho(z)} = \frac{\bar\rho(\bar z) + \delta\rho(\mathbf{n}, z) - \bar\rho(z)}{\bar\rho(z)} = \frac{\bar\rho(z - \delta z) + \delta\rho(\mathbf{n}, z) - \bar\rho(z)}{\bar\rho(z)} = \frac{\delta\rho(\mathbf{n}, z)}{\bar\rho(\bar z)} - \frac{d\bar\rho}{d\bar z}\frac{\delta z(\mathbf{n}, z)}{\bar\rho(\bar z)}. \quad (3)$$

Here $\bar z = \bar z(t)$ is the redshift of a background Friedmann universe that we compare our perturbation with and δz is the redshift perturbation to this universe. Moreover, $\rho(\mathbf{n}, \bar z(t)) = \bar\rho(t) + \delta\rho(\mathbf{n}, t)$, where the time is obtained by solving the background relation $\bar z = \bar z(t)$. Note that $\bar\rho(z) = \bar\rho(\bar z + \delta z)$ deviates to first order from $\bar\rho(\bar z)$. Clearly, both δz and $\delta\rho$ depend on the chosen background and are hence gauge dependent. However, their combination in Eq. (3) must turn out to be gauge invariant, as it is, in principle, observable.

Let us first compute the redshift in a perturbed Friedmann universe with metric

$$ds^2 = a^2(t)[-(1 + 2A)dt^2 - 2B_i dt dx^i + [(1 + 2H_L)\delta_{ij} + 2H_{Tij} + 2H_{ij}]dx^i dx^j]. \quad (4)$$

Here H_{ij} is the transverse traceless gravitational wave term and A, B_i, H_L, and H_{Tij} are scalar degrees of freedom, two of which can be removed by gauge transformations. In Fourier space $B_i = -\hat k_i B$ and $H_{Tij} = (\hat k_i\hat k_j - \delta_{ij}/3)H_T$. For simplicity, we shall neglect the contribution from gravitational waves in the main text. In Appendix A we also include these terms. We consider a photon emitted from a galaxy, the source, S, which is moving in direction $\mathbf{n}$ (hence, to lowest order, it is seen under the direction $-\mathbf{n}$ from the observer O). We denote the peculiar velocities of the source and observer by $\mathbf{v}_S$ and $\mathbf{v}_O$. The observer receives the photon redshifted by a factor

$$1 + z = \frac{(n\cdot u)_S}{(n\cdot u)_O}. \quad (5)$$

We solve the equation for the photon geodesic $n = a^{-2}(1 + \delta n^0, \mathbf{n} + \delta\mathbf{n})$, where $\mathbf{n}$ denotes the unperturbed photon direction at the observer. Using that $u = a^{-1}(1 - A, \mathbf{v})$, where $\mathbf{v}$ is the peculiar velocity, we find, by the same calculation which leads to Eq. (2.228) in [1] (see also [11]),

$$1 + z = \frac{a(t_O)}{a(t_S)}\left\{1 + \left[H_L + \frac{1}{3}H_T + \mathbf{n}\cdot\mathbf{V} + \Phi + \Psi\right]_{t_S}^{t_O} - \int_{r_S}^{0}(\dot\Phi + \dot\Psi)d\lambda\right\}. \quad (6)$$

The first term is simply $1 + \bar z$. Here t denotes conformal time, Ψ and Φ are the Bardeen potentials, and $\mathbf{V}$ is the gauge-invariant velocity perturbation which corresponds to the ordinary velocity perturbation in longitudinal gauge. For more details see [1,11] and Appendix A. In this redshift perturbation the dipole term $\mathbf{n}\cdot\mathbf{V}(\mathbf{x}_O, t_O)$ is the only term in the square brackets in (6) which depends on directions when evaluated at $\mathbf{x}_O$. The terms evaluated at the emission point do of course all depend on $\mathbf{n}$ via the position of the emission point which, to lowest order, is simply $\mathbf{x}_S = \mathbf{x}_O - \mathbf{n}(t_O - t(\bar z_S))$. The integral extends along the unperturbed photon trajectory from the emission point, where we set $\lambda = 0$, to our position where $\lambda = t_O - t_S = r_S$. Equation (6) implies that the redshift perturbation is

$$\delta z = z - \bar{z}$$
$$= -(1+z)\left[\left(H_L + \frac{1}{3}H_T + \mathbf{n}\cdot\mathbf{V} + \Phi + \Psi\right)(\mathbf{n}, z) + \int_0^{r_S}(\dot{\Phi} + \dot{\Psi})d\lambda\right], \quad (7)$$

where we have neglected the unmeasurable monopole term and the dipole term from the observer position. We indicate the source position by the direction it is seen under, $-\mathbf{n}$, and its observed redshift z. To lowest order $\mathbf{x}(\mathbf{n}, z) = -r_S(z)\mathbf{n}$. To obtain the density fluctuation in redshift space, we now use that $\frac{d\bar{\rho}}{d\bar{z}} = 3\frac{\bar{\rho}}{1+\bar{z}}$. With this we obtain

$$\delta_z(\mathbf{n}, z) = D_g(\mathbf{n}, z) + 3(\mathbf{V}\cdot\mathbf{n})(\mathbf{n}, z) + 3(\Psi + \Phi)(\mathbf{n}, z) + 3\int_{t_S}^{t_O}(\dot{\Psi} + \dot{\Phi})(\mathbf{n}, z(t))dt. \quad (8)$$

Here we relate a perturbation variable in direction $\mathbf{n}$ at redshift z to its unperturbed position and time, $f(\mathbf{n}, z) = f(\mathbf{x}(\mathbf{n}, z), t(z))$, and overdots are partial derivatives with respect to t, the second argument in $f(\mathbf{x}, t)$.

D_g is the density fluctuation on the uniform curvature hypersurface. It is related to the density fluctuation in comoving gauge, $D_{\rm cm}$, by [1,11]

$$D_{\rm cm} \equiv D = D_g + 3\Phi + 3k^{-1}\mathcal{H}V.$$

If we would want to introduce a bias between the matter density and the galaxy density, it would probably be most physical to assume that both galaxies and dark matter follow the same velocity field, as they experience the same gravitational acceleration. We then expect that biasing should be applied to the density fluctuation in comoving gauge, $D_{\rm cm}$, not to D_g. On small scales such differences are irrelevant, but on large scales they do become relevant, as becomes clear when considering the (linear) power spectra for the different density fluctuation variables; see Fig. 1.

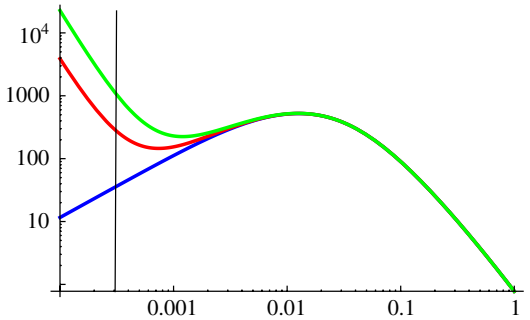

FIG. 1 (color online). The (linear) matter power spectrum on the uniform curvature hypersurface (top curve, green), in longitudinal gauge (middle curve, red), and in comoving gauge (bottom curve, blue).

B. Volume perturbations

As a next step we compute the volume perturbation $\delta V/V$ in Eq. (2), which must be gauge invariant since δ_z is also gauge invariant by itself. This is not surprising, as it would, in principle, be a measurable quantity if we had an "unbiased tracer" of the volume.

We consider a small volume element at the source position. By this we mean the spatial volume seen by a source with four-velocity u^μ. This is given by

$$dV = \sqrt{-g}\epsilon_{\mu\nu\alpha\beta}u^\mu dx^\nu dx^\alpha dx^\beta. \quad (9)$$

We want to express the volume element in terms of the polar angles at the observer position, θ_O and φ_O, and the observed redshift z. We have

$$dV = \sqrt{-g}\epsilon_{\mu\nu\alpha\beta}u^\mu\frac{\partial x^\nu}{\partial z}\frac{\partial x^\alpha}{\partial\theta_S}\frac{\partial x^\beta}{\partial\varphi_S}\left|\frac{\partial(\theta_S,\varphi_S)}{\partial(\theta_O,\varphi_O)}\right|dz d\theta_O d\varphi_O \equiv v(z,\theta_O,\varphi_O)dz d\theta_O d\varphi_O, \quad (10)$$

where we have introduced the density v which determines the volume perturbation,

$$\frac{\delta V}{V} = \frac{v - \bar{v}}{\bar{v}} = \frac{\delta v}{\bar{v}}.$$

$|\frac{\partial(\theta_S,\varphi_S)}{\partial(\theta_O,\varphi_O)}|$ is the determinant of the Jacobian of the transformation from the angles at the source to the angles at the observer. Equation (10) is still exact. In a homogeneous and isotropic universe geodesics are straight lines and $\theta_S = \theta_O$ and $\varphi_S = \varphi_O$. In a perturbed universe the angles at the source are perturbed with respect to the angles at the observer, and we have $\theta_S = \theta_O + \delta\theta$ and $\varphi_S = \varphi_O + \delta\varphi$. Hence to first order the Jacobian determinant becomes

$$\left|\frac{\partial(\theta_S,\varphi_S)}{\partial(\theta_O,\varphi_O)}\right| = 1 + \frac{\partial\delta\theta}{\partial\theta} + \frac{\partial\delta\varphi}{\partial\varphi}. \quad (11)$$

Using the expression for the metric determinant, $\sqrt{-g} = a^4(1 + A + 3H_L)$, and the four-velocity of the source, $u = \frac{1}{a}(1 - A, v^i)$, we find to first order

$$v = a^3(1 + A + 3H_L)\left[\frac{dr}{dz}r^2\sin\theta_S\left(1 + \frac{\partial\delta\theta}{\partial\theta} + \frac{\partial\delta\varphi}{\partial\varphi}\right) - \left(A\frac{d\bar{r}}{d\bar{z}} + v_r\frac{dt}{dz}\right)\bar{r}^2\sin\theta_O\right]. \quad (12)$$

Here dr/dz is to be understood as the change in comoving distance r with redshift along the photon geodesic. At linear order we can write (the distinction between z and $\bar{z}$ is only relevant for background quantities)

$$\frac{dr}{dz} = \frac{d\bar{r}}{d\bar{z}} + \frac{d\delta r}{d\bar{z}} - \frac{d\delta z}{d\bar{z}}\frac{d\bar{r}}{d\bar{z}} = \left(\frac{d\bar{r}}{dt} + \frac{d\delta r}{d\lambda} - \frac{d\delta z}{d\lambda}\frac{d\bar{r}}{d\bar{z}}\right)\frac{dt}{d\bar{z}}, \quad (13)$$

where we have used that for first order quantities we can set $dt = d\lambda$ when we have to take the derivative along the photon geodesic. The last term of Eq. (13) contains the

redshift-space distortion which will turn out to be the biggest correction to the power spectrum. To lowest order along a photon geodesic $-d\bar{r}/d\bar{z} = dt/d\bar{z} = -H^{-1} = -a/\mathcal{H}$, where H is the physical Hubble parameter and $\mathcal{H} = aH$ is the comoving Hubble parameter. With this the volume element becomes

$$v = \frac{a^4\bar{r}^2\sin\theta_O}{\mathcal{H}}\Big[1 + 3H_L + \Big(\cot\theta_O + \frac{\partial}{\partial\theta}\Big)\delta\theta + \frac{\partial\delta\varphi}{\partial\varphi} - \mathbf{v}\cdot\mathbf{n} + \frac{2\delta r}{r} - \frac{d\delta r}{d\lambda} + \frac{a}{\mathcal{H}}\frac{d\delta z}{d\lambda}\Big]. \quad (14)$$

To obtain the fluctuation of v we subtract the unperturbed part $\bar{v}(z)$. Note, however, that we evaluate this at the observed redshift, $z = \bar{z} + \delta z$. Hence

$$\bar{v}(z) = \bar{v}(\bar{z}) + \frac{d\bar{v}}{d\bar{z}}\delta z.$$

From the unperturbed expression with $a = 1/(\bar{z}+1)$,

$$\bar{v}(\bar{z}) = \frac{\sin\theta_O\bar{r}^2}{(1+\bar{z})^4\mathcal{H}}, \quad (15)$$

one infers

$$\frac{d\bar{v}}{d\bar{z}} = \bar{v}(\bar{z})\Big(-4 + \frac{2}{\bar{r}_S\mathcal{H}} + \frac{\dot{\mathcal{H}}}{\mathcal{H}^2}\Big)\frac{1}{1+\bar{z}}. \quad (16)$$

Combining Eqs. (14) and (16) we obtain for the perturbation of the volume element

$$\frac{\delta v}{\bar{v}}(\mathbf{n}, z) = \frac{v(z) - \bar{v}(z)}{\bar{v}(z)} = 3H_L + \Big(\cot\theta_O + \frac{\partial}{\partial\theta}\Big)\delta\theta + \frac{\partial\delta\varphi}{\partial\varphi} - \mathbf{v}\cdot\mathbf{n} + \frac{2\delta r}{r} - \frac{d\delta r}{d\lambda} + \frac{1}{\mathcal{H}(1+\bar{z})}\frac{d\delta z}{d\lambda} - \Big(-4 + \frac{2}{\bar{r}\mathcal{H}} + \frac{\dot{\mathcal{H}}}{\mathcal{H}^2}\Big)\frac{\delta z}{1+\bar{z}}. \quad (17)$$

In order to express these quantities in terms of the perturbed metric and the peculiar velocity of observer and emitter, we need to compute the deviation vector that relates the perturbed geodesic to the unperturbed one, $\delta x^\mu(\lambda) = x^\mu(\lambda) - \bar{x}^\mu(\lambda)$. Here we give only the main steps. More details on the derivation can be found in Appendix A. We use

$$\frac{dx^\mu}{dt} = \frac{dx^\mu}{d\lambda}\frac{d\lambda}{dt} = \frac{n^\mu}{n^0} \quad (18)$$

which leads to

$$x^0(t_S) = -(t_O - t_S) = r_S \text{ at every order,} \quad (19)$$

$$x^i(t_S) = -(t_O - t_S)\bar{n}^i - \int_0^{r_S} d\lambda(\delta n^i - \bar{n}^i\delta n^0) \quad (20)$$

to first order.

In the following we neglect perturbations at the observer position since, as already mentioned, they give rise only to an unmeasurable monopole term or a dipole term. Using the null geodesic equation for n^μ we find

$$\delta x^i(t_S) = \int_0^{r_S} d\lambda(h_{\alpha i}\bar{n}^\alpha + h_{0\alpha}\bar{n}^i\bar{n}^\alpha) + \frac{1}{2}\int_0^{r_S} d\lambda(r_S - r)(h_{\alpha\beta,i} + \dot{h}_{\alpha\beta}\bar{n}^i)\bar{n}^\alpha\bar{n}^\beta, \quad (21)$$

where $r(\lambda) = \lambda$. From this we obtain

$$\delta r \equiv \delta x^i e_{ri} = -\delta x^i\bar{n}_i = -\frac{1}{2}\int_0^{r_S} d\lambda h_{\alpha\beta}\bar{n}^\alpha\bar{n}^\beta = \int_0^{r_S} d\lambda(\Phi + \Psi) + \frac{B}{k} + \frac{1}{k^2}\Big(\frac{dH_T}{d\lambda} - 2\dot{H}_T\Big). \quad (22)$$

We also use that $\bar{n}^i\partial_i + \partial_t = \frac{d}{d\lambda} = \frac{d}{dt}$ and $r_S = t_O - t_S$ to lowest order. For the derivative of δr we obtain

$$\frac{d\delta r}{d\lambda} = -(\Phi + \Psi) + \frac{1}{k}\frac{dB}{d\lambda} + \frac{1}{k^2}\Big(\frac{d^2H_T}{d\lambda^2} - 2\frac{d\dot{H}_T}{d\lambda}\Big). \quad (23)$$

Similarly we find for the perturbed angles

$$\delta\theta \equiv \frac{\delta x^i e_{\theta i}}{r_S} = \frac{1}{r_S}\int_0^{r_S} d\lambda\Big(h_{\alpha i}\bar{n}^\alpha e^i_\theta + \frac{1}{2}(r_S - r)h_{\alpha\beta,i}e^i_\theta\bar{n}^\alpha\bar{n}^\beta\Big), \quad (24)$$

$$\delta\varphi \equiv \frac{\delta x^i e_{\varphi i}}{r_S\sin\theta_O} = \frac{1}{r_S\sin\theta_O}\int_0^{r_S} d\lambda\Big(h_{\alpha i}\bar{n}^\alpha e^i_\varphi + \frac{1}{2}(r_S - r)h_{\alpha\beta,i}e^i_\varphi\bar{n}^\alpha\bar{n}^\beta\Big). \quad (25)$$

We have used that $\bar{n}^i e_{\theta i} = \bar{n}^i e_{\varphi i} = 0$. The second term of the integral in Eq. (24) can be rewritten as

$$h_{\alpha\beta,i}e^i_\theta\bar{n}^\alpha\bar{n}^\beta = \frac{1}{r}\partial_\theta(h_{\alpha\beta})\bar{n}^\alpha\bar{n}^\beta = \frac{1}{r}[\partial_\theta(h_{\alpha\beta}\bar{n}^\alpha\bar{n}^\beta) - h_{\alpha\beta}\partial_\theta(\bar{n}^\alpha\bar{n}^\beta)], \quad (26)$$

where $\partial_\theta\bar{n}^\alpha = -e^i_\theta\delta_{i\alpha}$, and analogously for φ. The angular contribution to the volume then reads

$$
\begin{aligned}
&(\cot\theta + \partial_\theta)\delta\theta + \partial_\varphi \delta\varphi \\
&= \int_0^{r_S} d\lambda \frac{(r_S - r)}{2 r_S r}\left[\cot\theta\partial_\theta + \partial_\theta^2 + \frac{1}{\sin^2\theta}\partial_\varphi^2\right] h_{\alpha\beta}\bar{n}^\alpha\bar{n}^\beta \\
&\quad + \int_0^{r_S} d\lambda \frac{1}{r}\left[(\cot\theta + \partial_\theta) h_{i\alpha} e^i_\theta \bar{n}^\alpha + \frac{\partial_\varphi}{\sin\theta} h_{i\alpha} e^i_\varphi \bar{n}^\alpha\right] \\
&= \frac{-1}{r_S}\int_0^{r_S} d\lambda \frac{(r_S - r)}{r}\Delta_\Omega(\Phi + \Psi) - \frac{\Delta_\Omega H_T(t_S)}{k^2 r_S^2}, \qquad (27)
\end{aligned}
$$

where Δ_Ω denotes the angular part of the Laplacian,

$$
\Delta_\Omega \equiv \left(\cot\theta\partial_\theta + \partial_\theta^2 + \frac{1}{\sin^2\theta}\partial_\varphi^2\right). \qquad (28)
$$

It is interesting to note that the angular part of the volume perturbation is not a gauge-invariant quantity by itself. If $H_T \neq 0$ the angular and radial directions are mixed in a nontrivial way. This is not really surprising since the angular volume distortion is not a measurable quantity by itself. On the other hand, the convergence κ and the magnification μ that are observable contain, in addition to the angular volume distortion, other perturbations (see [12,13]) and are gauge invariant.

The redshift contribution to the volume perturbation is obtained by differentiating Eq. (7).

$$
\begin{aligned}
\frac{1}{\mathcal{H}(1+\bar{z})}\frac{d\delta z}{d\lambda} &= \Phi + \Psi + H_L + \frac{H_T}{3} + \mathbf{V}\cdot\mathbf{n} \\
&\quad + \int_0^{r_S} d\lambda(\dot{\Phi} + \dot{\Psi}) - \frac{1}{\mathcal{H}}\left(\bar{n}^i\partial_i(\Phi + \Psi)\right. \\
&\quad \left. + \frac{dH_L}{d\lambda} + \frac{1}{3}\frac{dH_T}{d\lambda} + \frac{d(\mathbf{V}\cdot\mathbf{n})}{d\lambda}\right). \qquad (29)
\end{aligned}
$$

Putting everything together we find, after several integrations by part and a total Laplacian of H_T which cancels a factor $1/k^2$, the following expression for the volume density perturbation:

$$
\begin{aligned}
\frac{\delta v}{v} &= -2(\Psi + \Phi) - 4\mathbf{V}\cdot\mathbf{n} + \frac{1}{\mathcal{H}}\left[\dot{\Phi} + \partial_r\Psi - \frac{d(\mathbf{V}\cdot\mathbf{n})}{d\lambda}\right] \\
&\quad + \left(\frac{\dot{\mathcal{H}}}{\mathcal{H}^2} + \frac{2}{r_S\mathcal{H}}\right)\left(\Psi + \mathbf{V}\cdot\mathbf{n} + \int_0^{r_S} d\lambda(\dot{\Phi} + \dot{\Psi})\right) \\
&\quad - 3\int_0^{r_S} d\lambda(\dot{\Phi} + \dot{\Psi}) + \frac{2}{r_S}\int_0^{r_S} d\lambda(\Phi + \Psi) \\
&\quad - \frac{1}{r_S}\int_0^{r_S} d\lambda \frac{r_S - r}{r}\Delta_\Omega(\Phi + \Psi). \qquad (30)
\end{aligned}
$$

Here and in the following, the functions without arguments are to be evaluated at the source position $\mathbf{x}_S = \mathbf{x}_O - \mathbf{n}(t_O - t_S)$ and at the source time t_S. More details of the derivation of this result are given in Appendix A.

Adding the results (8) and (30) we obtain the galaxy number density fluctuation in redshift space as defined in Eq. (2),

$$
\begin{aligned}
\Delta(\mathbf{n}, z) &= D_g + \Phi + \Psi + \frac{1}{\mathcal{H}}[\dot{\Phi} - \partial_r(\mathbf{V}\cdot\mathbf{n})] \\
&\quad + \left(\frac{\dot{\mathcal{H}}}{\mathcal{H}^2} + \frac{2}{r_S\mathcal{H}}\right)\left(\Psi + \mathbf{V}\cdot\mathbf{n} + \int_0^{r_S} d\lambda(\dot{\Phi} + \dot{\Psi})\right) \\
&\quad + \frac{1}{r_S}\int_0^{r_S} d\lambda\left[2 - \frac{r_S - r}{r}\Delta_\Omega\right](\Phi + \Psi). \qquad (31)
\end{aligned}
$$

Here we have used that pressureless matter also moves along geodesics so that

$$
\mathbf{n}\cdot\dot{\mathbf{V}} + \mathcal{H}\mathbf{n}\cdot\mathbf{V} - \partial_r\Psi = 0.
$$

Equation (31) together with (8) and (30) is our first main result.

The first term in (31) is the gauge-invariant density fluctuation. D_g is the density fluctuation in the flat slicing. It is related to the density perturbation in Newtonian gauge by $D_g = D_s - 3\Phi$. In terms of D_s the first three contributions combine to form $D_g + \Phi + \Psi = D_s - 2\Phi + \Psi$.

The term $-\mathcal{H}^{-1}\partial_r(\mathbf{n}\cdot\mathbf{V})$ is the redshift-space distortion. As we shall see in the next section, this is the largest single correction on intermediate scales. The second line comes from the redshift perturbation of the volume. It contains a Doppler term and the ordinary and integrated Sachs-Wolfe terms. The third line represents the radial and angular volume distortions. The second term in the integral on the third line is especially relevant on large scales; it is the lensing distortion.

III. THE ANGULAR POWER SPECTRUM OF THE GALAXY DENSITY FLUCTUATIONS

For fixed redshift, $\Delta(z, \mathbf{n})$ is a function on the sphere and it is most natural to expand it in spherical harmonics. Let us do this with the result (31),

$$
\Delta(\mathbf{n}, z) = \sum_{\ell m} a_{\ell m}(z) Y_{\ell m}(\mathbf{n}), \qquad C_\ell(z) = \langle |a_{\ell m}|^2\rangle. \qquad (32)
$$

The coefficients $a_{\ell m}(z)$ are given by

$$
a_{\ell m}(z) = \int d\Omega_{\mathbf{n}} Y^*_{\ell m}(\mathbf{n})\Delta(\mathbf{n}, z). \qquad (33)
$$

The star indicates complex conjugation.

The different terms in $\Delta(\mathbf{n}, z)$ are either a perturbation variable evaluated at the source position or an integral of a perturbation variable over the unperturbed photon trajectory. Let us first consider a contribution from a perturbation variable at the source position, e.g. Ψ. We want to relate the $C_\ell(z)$ spectra to the usual power spectrum $P_\Psi(k, t)$ which is defined by

$$
\langle\Psi(\mathbf{k}, t)\Psi^*(\mathbf{k}', t)\rangle = (2\pi)^3\delta(\mathbf{k} - \mathbf{k}')P_\Psi(k, t).
$$

The delta function and the fact that P_Ψ depends only on the modulus of $\mathbf{k}$, $k \equiv |\mathbf{k}|$, are a consequence of statistical homogeneity and isotropy. Expressing Ψ in terms of its Fourier transform,

$$\Psi(\mathbf{x}, t) = \frac{1}{(2\pi)^3} \int d^3k \Psi(\mathbf{k}, t) e^{-i(\mathbf{k}\cdot\mathbf{x})},$$

a short calculation (see e.g. [1]) gives

$$a^{\Psi}_{\ell m}(z_S) = \frac{i^\ell}{2\pi^2} \int d^3k j_\ell(kr_S)\Psi(\mathbf{k}, t_S) Y^*_{\ell m}(\hat{\mathbf{k}}). \quad (34)$$

Here j_ℓ is the spherical Bessel function of order ℓ; see [14]. Correspondingly, the contribution from an integral $\int_0^{r_S} f(\mathbf{x}(\lambda), t(\lambda))d\lambda$ becomes

$$a^{\int f}_{\ell m}(z_S) = \frac{i^\ell}{2\pi^2} \int_0^{r_S} d\lambda \int d^3k j_\ell(k\lambda) f(\mathbf{k}, t) Y^*_{\ell m}(\hat{\mathbf{k}}). \quad (35)$$

For a velocity term $\mathbf{V}\cdot\mathbf{n}$ we use that $\mathbf{V}(\mathbf{k}, t) = i\hat{\mathbf{k}}V$, so that $\mathbf{V}\cdot\mathbf{n}\exp[i(\mathbf{k}\cdot\mathbf{n})r] = V\partial_{kr}\exp[i(\mathbf{k}\cdot\mathbf{n})r]$. With this, one obtains

$$a^{\mathbf{Vn}}_{\ell m}(z_S) = \frac{i^\ell}{2\pi^2} \int d^3k j'_\ell(kr_S) V(\mathbf{k}, t) Y^*_{\ell m}(\hat{\mathbf{k}}). \quad (36)$$

The prime in j_ℓ denotes a derivation with respect to the argument. Finally, for the redshift-space distortion, $-\partial_r(\mathbf{V}\cdot\mathbf{n}) = \mathbf{n}\cdot\boldsymbol{\nabla}(\mathbf{V}\cdot\mathbf{n})$, we have to use the above identity twice and arrive at

$$a^{-\partial_r(\mathbf{Vn})}_{\ell m}(z_S) = \frac{i^\ell}{2\pi^2} \int d^3k j''_\ell(kr_S) k^{-1} V(\mathbf{k}, t) Y^*_{\ell m}(\hat{\mathbf{k}}). \quad (37)$$

One can now write down the $C_\ell(z)$'s for one's theory of choice for the background and the perturbations, e.g. for modified gravity or a quintessence model.

So far the derivation has been completely general. We have not used Einstein's equation. The only assumptions are that galaxies follow the distribution of matter which is made out of nonrelativistic particles which move along geodesics, and that photons move along null geodesics.

To proceed further, we have to be more specific. Here we just study the simplest model of purely *scalar adiabatic perturbations*, which have been generated at some early time in the past (e.g. inflation). If there are more e.g. isocurvature modes present, the subsequent calculation has to be repeated for them.

In the case of one adiabatic mode, all the perturbation variables are given by transfer functions from some initial random variable that we take to be the Bardeen potential Ψ. Hence

$$\Psi(\mathbf{k}, t) = T_\Psi(k, t)\Psi_{\rm in}(\mathbf{k}), \quad (38)$$

$$\Phi(\mathbf{k}, t) = T_\Phi(k, t)\Psi_{\rm in}(\mathbf{k}), \quad (39)$$

$$D_g(\mathbf{k}, t) = T_D(k, t)\Psi_{\rm in}(\mathbf{k}), \quad (40)$$

$$V(\mathbf{k}, t) = T_V(k, t)\Psi_{\rm in}(\mathbf{k}). \quad (41)$$

The transfer functions $T_\bullet$ depend on the matter content and the evolution history of the Universe and on the theory of gravity which relates matter and metric degrees of freedom. What is important for us is that they are deterministic functions and do not depend on directions of $\mathbf{k}$. We characterize the initial power spectrum by a spectral index n and an amplitude A,

$$k^3\langle\Psi_{\rm in}(\mathbf{k})\Psi^*_{\rm in}(\mathbf{k}')\rangle = (2\pi)^3\delta(\mathbf{k}-\mathbf{k}')A(kt_O)^{n-1}. \quad (42)$$

We have introduced present time t_O in order to keep A dimensionless. From the CMB observations we know that it is of the order of $A \sim 10^{-8}$. With these identifications we can now relate $C_\ell(z)$ to the initial power spectrum $A(kt_O)^{n-1}$. Inserting the above in expression (31), a short calculation gives

$$C_\ell(z_S) = \frac{2A}{\pi} \int \frac{dk}{k} (kt_O)^{n-1} |F_\ell(k, z_S)|^2 \quad (43)$$

with

$$F_\ell(k, z_S) = j_\ell(kr_S)\left[T_D + \left(1 + \frac{\dot{\mathcal{H}}}{\mathcal{H}^2} + \frac{2}{r_S\mathcal{H}}\right)T_\Psi + T_\Phi + \frac{1}{\mathcal{H}}\dot{T}_\Phi\right] + j'_\ell(kr_S)\left(\frac{\dot{\mathcal{H}}}{\mathcal{H}^2} + \frac{2}{r_S\mathcal{H}}\right)T_V + \frac{k}{\mathcal{H}}T_V j''_\ell(kr_S)$$
$$+ \frac{1}{r_S}\int_0^{r_S} j_\ell(k\lambda)\left(2 + \frac{r_S-\lambda}{\lambda}\ell(\ell+1)\right)(T_\Psi + T_\Phi)d\lambda + \left(\frac{\dot{\mathcal{H}}}{\mathcal{H}^2} + \frac{2}{r_S\mathcal{H}}\right)\int_0^{r_S} j_\ell(k\lambda)(\dot{T}_\Psi + \dot{T}_\Phi)d\lambda. \quad (44)$$

Here $r_S = t_O - t_S$ is the source position.

We now evaluate and compare the amplitude of different terms in a ΛCDM universe. Rather than entering in a precise numerical evaluation, we estimate the terms by using approximations for the transfer functions. This will help us to gain insight into the importance of the different terms. We plan to do a full numerical evaluation which can be used to estimate cosmological parameters in future work.

From the first order Einstein equations, neglecting anisotropic stresses from neutrinos, we can relate the transfer functions T_D, T_V, and T_Φ to T_Ψ. We find

$$T_\Phi = T_\Psi, \quad (45)$$

$$T_D = -\frac{2a}{3\Omega_m}\left(\frac{k}{\mathcal{H}_0}\right)^2 T_\Psi - 3T_\Psi - 3\frac{\mathcal{H}}{k}T_V, \quad (46)$$

$$T_V = \frac{2a}{3\Omega_m}\frac{k}{\mathcal{H}_0^2}(\mathcal{H}T_\Psi + \dot{T}_\Psi). \quad (47)$$

Using the notation of [15] (see also [16]), we decompose the transfer function $T_\Psi(k, t)$ into a growth rate $D_1(a)$ and a time independent transfer function $T(k)$ such that

$$T_\Psi(k, t) = \frac{9}{10}\frac{D_1(a)}{a}T(k), \tag{48}$$

and we use CAMBCODE [17] to compute $T(k)$. The amplitude of the power spectrum can be expressed as [15] $A = \frac{50\pi^2}{9}\delta_H^2(\frac{\Omega_m}{D_1(a=1)})^2$. We choose $\Omega_m = 0.24$, $\Omega_\Lambda = 0.76$, and $\sigma_8 = 0.75$, leading to $\delta_H = 5.6 \times 10^{-5}$.

A. The transversal power spectrum

Let us first determine the C_ℓ's at fixed redshift. They provide the transversal power spectrum, i.e. correlations on the sphere normal to the observer directions. Of course for the intrinsic density fluctuations these are not different from correlations in any other direction, but observational effects on them are different. For example, as we can only observe on the background light cone, we can only see fluctuations on this sphere at the same time but not fluctuations which have a different radial distance from us. On the other hand, in general, the same redshift does of course not imply the same lookback time, since both these quantities are perturbed in different ways.

In Fig. 2 (top panel) we show the total transversal power spectrum at redshifts $z_S = 0.1$, 0.5, 1, and 3. Note that the amplitude of the linear power spectrum from $z_S = 0.1$ to $z_S = 0.5$ is reduced by a factor 6 at $\ell \sim 100$ and by a factor 20 at $\ell \lesssim 10$. This comes from the following fact: the transversal power spectrum is dominated by the density fluctuation and the redshift-space distortion which are proportional to integrals of the form

$$\int \frac{dk}{k}\left(\frac{k}{\mathcal{H}_0}\right)^4 T^2(k) j_\ell^2(kr_S).$$

At $x = kr_S = \ell$, this term goes like ℓ^4 and it is therefore expected to dominate at large ℓ. However, since for a constant transfer function, this integral would diverge, it is dominated by the maximum of the transfer function which is roughly at $k_{\rm eq}$. Since for $z \gtrsim 0.5$, $k_{\rm eq} r_S \gtrsim \ell$, $j_\ell^2(k_{\rm eq} r_S) \propto 1/(k_{\rm eq} r_S)^2$ which therefore decreases like $1/r_S^2$. Already this simple observation tells us that the amplitude of the transversal power spectrum at different redshifts might offer a possibility to constrain $r_S(z)$ and the growth factor, which both depend on cosmological parameters in different ways. On the other hand, this is complicated by nonlinear effects and biasing which are not accounted for in this work.

The different contributions to the power spectrum at different redshifts are shown in more detail in Fig. 3. For $z_S = 1$, we show the spectrum up to $\ell = 600$ while for the other redshifts we stop at $\ell = 100$, beyond which

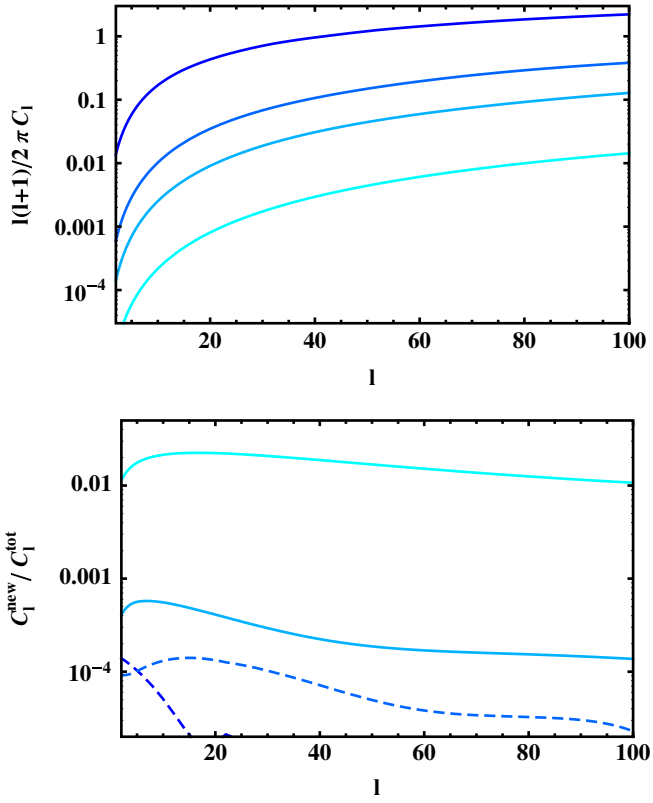

FIG. 2 (color online). Top panel: The transversal power spectrum at (from top to bottom) $z_S = 0.1$, $z_S = 0.5$, $z_S = 1$, and $z_S = 3$. Bottom panel: The ratio between the new contributions (lensing + potential) and the total angular power spectrum at (from top to bottom) $z_S = 3$, $z_S = 1$, $z_S = 0.5$, and $z_S = 0.1$. Solid lines denote positive contributions whereas dashed lines denote negative contributions.

the structure does not change anymore. We denote by D the density term in comoving gauge,

$$D = D_g + 3\Phi + 3\frac{\mathcal{H}}{k}V,$$

by z the redshift-space distortion, by L the lensing term, by V the Doppler terms, and by Ψ the gravitational potential terms (see Table I for a definition of each term). C_ℓ^{DD} represents, for example, the contribution from the density term alone and C_ℓ^{Dz} the correlation between the density and redshift-space distortion. Except for the correlation between the density and redshift-space distortion that we represent individually, we include the correlations with the smaller contribution. Note that usually the correlations between lensing, Doppler, and gravitational potential are negligible and, except when explicitly specified, we do neglect them. Therefore, when we plot, for example, the lensing term (magenta), it contains $C_\ell^{LL} + 2C_\ell^{LD} + 2C_\ell^{Lz}$. The formulas for the dominant C_ℓ's are given in Appendix B.

The lensing term scales like ℓ^4 and is, in principle, of the same order as the density and redshift-space distortion

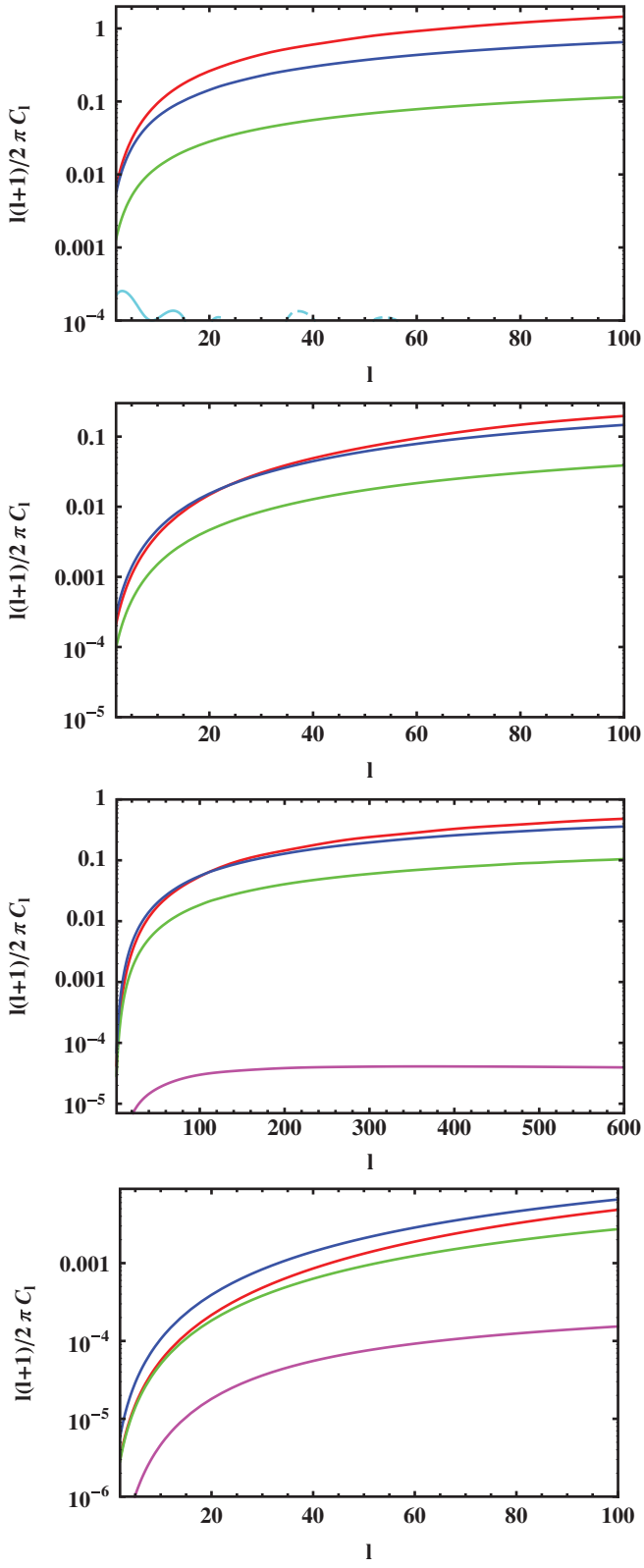

FIG. 3 (color). The dominant terms at redshifts (from top to bottom) $z_S = 0.1$, 0.5, 1, and 3: density (red line), redshift-space distortion (green line), the correlation of density with redshift-space distortion (blue line), lensing (magenta line), and Doppler (cyan line); see Table I. The potential terms are too small to appear on our log-plot.

TABLE I. The color coding of the different terms of Eq. (31) in the angular power spectrum of $\Delta(\mathbf{n}, z)$ as shown in Figs. 3–5, 7, 9, and 10. In addition to the terms given in the second column, all the correlations with the terms in the lines above are also included. Only the most dominant correlation between density and redshift-space distortion is shown separately in blue. In Figs. 5 and 10 the "standard terms," i.e. the top three lines, are represented together as the blue line.

Density	D	Red
Redshift-space distortion	$-\mathcal{H}^{-1}\partial_r(\mathbf{V}\cdot\mathbf{n})$	Green
Lensing	$\frac{-1}{r_S}\int_0^{r_S} d\lambda \frac{r_S - r}{r}\Delta_\Omega(\Phi+\Psi)$	Magenta
Correlation	$-2D\mathcal{H}^{-1}\partial_r(\mathbf{V}\cdot\mathbf{n})$	Blue
Doppler	$(\frac{\dot{\mathcal{H}}}{\mathcal{H}^2}+\frac{2}{r_S\mathcal{H}})\mathbf{V}\cdot\mathbf{n}$	Cyan
Potential	$\Psi - 2\Phi + \frac{2}{r_S}\int_0^{r_S} d\lambda(\Phi+\Psi) + (\frac{\dot{\mathcal{H}}}{\mathcal{H}^2}+\frac{2}{r_S\mathcal{H}})[\Psi + \int_0^{r_S} d\lambda(\dot{\Phi}+\dot{\Psi})] - \frac{2a}{\Omega_m}(\frac{\mathcal{H}}{\mathcal{H}_0})^2(\Psi+\frac{\Phi}{\mathcal{H}})$	Black

terms. However, it is given by an integral of the form (see Appendix B)

$$\frac{\ell^2(\ell+1)^2}{r_S^2}\int\frac{dk}{k}T^2(k)\left[\int_0^{r_S} d\lambda\,\frac{r_S - r}{r}j_\ell(kr)\right]^2$$

which does converge when integrated over k. It is therefore dominated at $k = \ell/r$. (We have used Limber's approximation [18] to evaluate this integral, which we have tested numerically and found to be of excellent accuracy.) The contribution of the lensing term becomes more important at larger source redshift for small ℓ. But it always remains subdominant in the transversal power spectrum. In the bottom panel of Fig. 2 we plot the ratio between the new contributions, i.e. lensing term plus potential term, and the total angular power spectrum. We see that neglecting the new contributions for $z_S \leq 1$ represents an error of no more than 0.1%, whereas for $z_S = 3$ the error amounts to a few percent. Note that we do not include the Doppler terms in the new contributions since they appear already in the original Kaiser formula [19] (even though there the term from expansion $\propto \dot{\mathcal{H}}/\mathcal{H}^2$, which is of the same order for redshifts $z \geq 1$, is not considered). In Fig. 4 (top panel) we depict the redshift dependence of all the terms for a fixed value of $\ell = 20$. The lensing and potential terms are both negative at small redshift and become positive at large redshift. This is due to the fact that at small redshift the dominant contribution comes from their correlation with the density that is negative, whereas at large redshift the dominant contribution is their autocorrelation, C_ℓ^{LL}, respectively $C_\ell^{\Psi\Psi}$. The bottom panel of Fig. 4 shows the ratio between the new contributions and the total angular power spectrum. The error induced by neglecting the new terms increases with redshift and it reaches a few percent at high redshift.

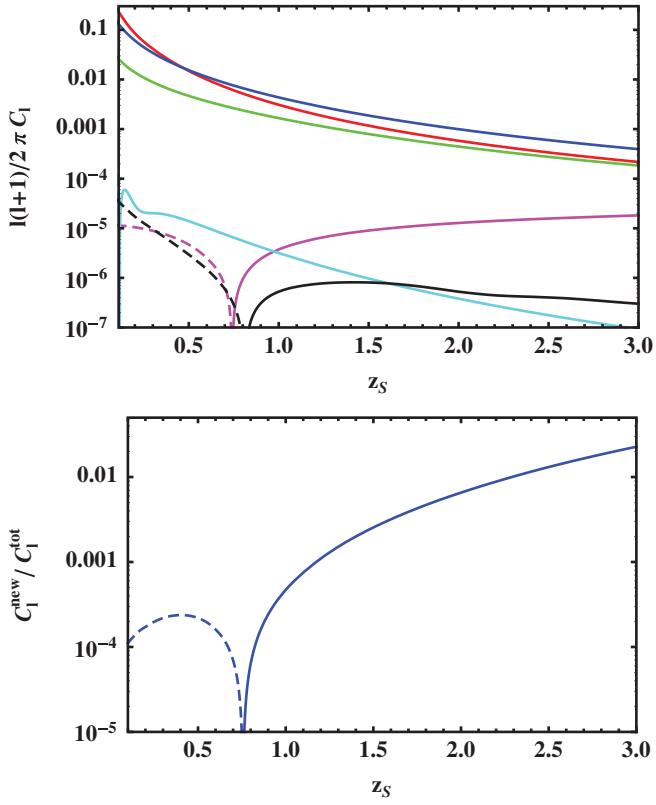

FIG. 4 (color). Top panel: The various terms as a function of z_S for a fixed value of $\ell = 20$: density (red line), redshift-space distortion (green line), the correlation of density with redshift-space distortion (blue line), lensing (magenta line), Doppler (cyan line), and potential (black line); see Table I. Solid lines denote positive contributions whereas dashed lines denote negative contributions. Bottom panel: The ratio between the new contributions (lensing + potential) and the total angular power spectrum as a function of z_S for a fixed value of $\ell = 20$.

B. The radial power spectrum

The results above give us the transversal power spectrum at fixed redshift. But of course there is also a radial power spectrum which correlates fluctuation at different distances from us. This encodes different information, and it is important to study them both. From the fact that the transfer function is not direction dependent, we infer that

$$\langle a_{\ell m}(z_S) a_{\ell' m'}(z_{S'})\rangle = \delta_{\ell,\ell'}\delta_{m,m'} C_\ell(z_S, z_{S'}). \quad (49)$$

Hence the radial power spectrum is given by

$$C_\ell(z_S, z_{S'}) = \frac{2A}{\pi}\int \frac{dk}{k}(kt_O)^{n-1} F_\ell(k, z_S) F^*_\ell(k, z_{S'}). \quad (50)$$

Here an interesting new phenomenon occurs: due to the fact that we evaluate $F_\ell(k, z_S)$ at different redshifts, we also evaluate the Bessel functions $j_\ell(kr_S)$ at different distances r_S. This leads to a suppression of the result due to oscillations, if the region in k space where the integrand dominates has $kr_S > \ell$. As we discussed above, this is the case for the k^2 term of the density fluctuations and for the redshift-space distortion, the terms which dominate the transversal power spectrum. These terms are therefore substantially suppressed in the radial power spectrum. All other terms have convergent integrals of $j^2_\ell(kr_S)$, already when neglecting the turnover of the transfer function; hence they are suppressed by powers of ℓ with respect to the lensing term. Therefore the lensing term dominates the radial power spectrum at low ℓ. This is precisely what one sees in Fig. 5, where the lensing term (magenta) dominates for $z_{S'}$ significantly larger than z_S. As in Fig. 4, at small redshift $z_S = 0.1$ and $z_S = 0.5$, the correlation density lensing dominates (and is negative), whereas at large redshift $z_S = 3$ the lensing-lensing term dominates. It is interesting to note how constant the lensing term remains, while the density term and the redshift-space distortion decay very rapidly with growing redshift difference. At $z_S = 1$ the lensing-lensing term and its correlation with the density are of the same order of magnitude which explains the change of sign as $z_{S'}$ increases. Finally, at $z_S = 0.1$ the Doppler term dominates over the standard term for some very specific values of $z_{S'}$. The first of them is actually the zero in the real space correlation function which e.g. at redshift $z_S = 0.1$ corresponds to $\delta z = 0.011$.

An alternative way to measure radial correlations is to introduce a window function $W(z, z')$ which corresponds to a smearing of fluctuations on scales smaller than some width Δz_S. We use a Gaussian window around some mean redshift z_S with width Δz_S. This suppresses power which comes from values of k with $k\Delta r_S > \ell$, where $\Delta r_S = r(z_S + \Delta z_S) - r(z_S)$. This is also a more realistic case since we can measure the galaxy distribution only in redshift bins of some finite width. A small width does already substantially affect the resulting spectrum of the density (see Fig. 6, top panel) and the redshift-space distortion (middle panel). As expected, the lensing term is insensitive to this smearing (bottom panel).

In Fig. 7 we show the effect of a 10% window on the different terms at different redshifts. As before, the terms which we indicate by "lensing term," "Doppler term," and "gravitational potential contributions" in the figure are not only the corresponding terms themselves but also their correlations with all other terms. If the latter dominate, such a contribution can become negative. For example, the lensing contribution for $z_S = 1$ changes sign at $\ell = 28$. For $\ell > 28$ it is dominated by negative correlations with the density, while for $\ell < 28$ the positive autocorrelation dominates. Since the power from scales smaller than $k\Delta r_S$ is removed, the power at ℓ truly corresponds to that at $k = \ell/r(z)$ in the power spectrum. The "wiggles" in the density and in the velocity terms for $z_S = 0.1$ are the baryon acoustic oscillations, the first of which appears at $\ell \simeq 15$ for $z_S = 0.1$. They are also visible in the anticorrelation of the lensing term with the density for $z_S = 0.5$ and

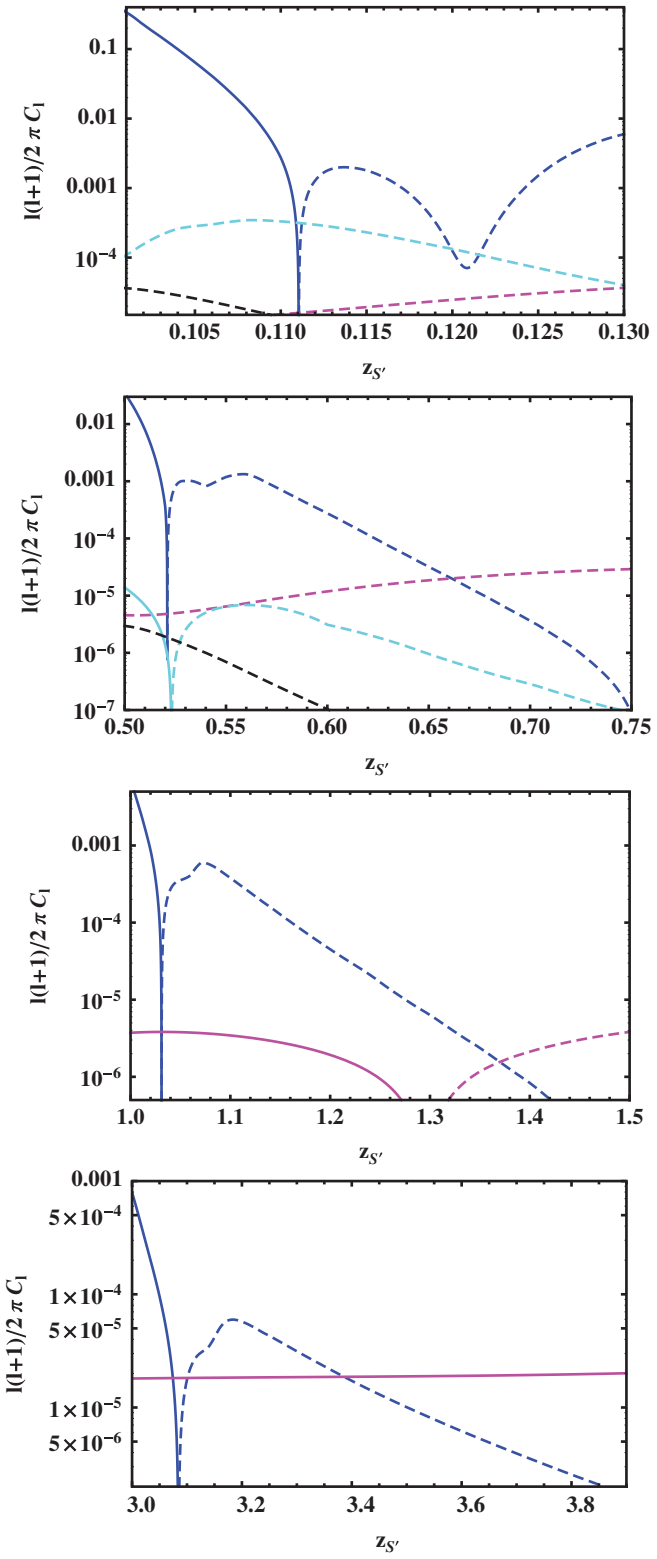

FIG. 5 (color). Different terms of $C_\ell(z_S, z_{S'})$ at $\ell = 20$ for redshifts (from top to bottom) $z_S = 0.1$, 0.5, 1, and 3, plotted as a function of $z_{S'}$: standard term, i.e. $C_\ell^{DD} + C_\ell^{zz} + 2C_\ell^{Dz}$ (blue line), lensing (magenta line), Doppler (cyan line), and potential (black line); see Table I. Solid lines denote positive contributions whereas dashed lines denote negative contributions.

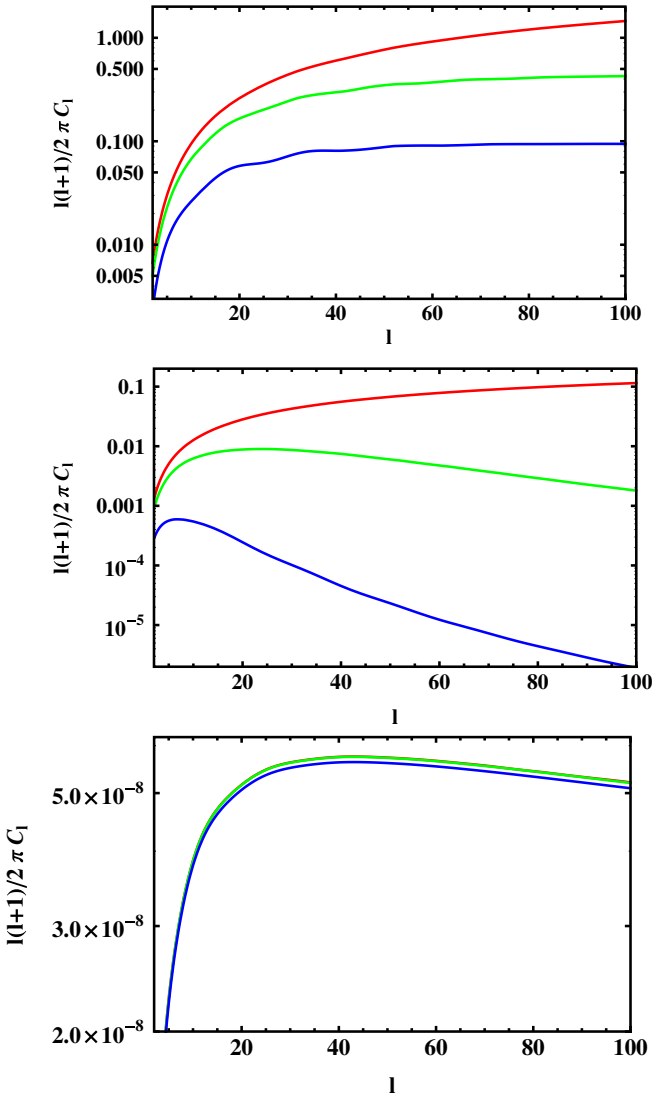

FIG. 6 (color online). The effect of a window function on the density contribution (top panel), redshift-space distortion (middle panel), and lensing contribution (bottom panel). We have chosen $z_S = 0.1$ and $\Delta z_S = 0$ (no window, top curve, red), $\Delta z_S = 0.002$ (middle curve, green), and $\Delta z_S = 0.01$ (bottom curve, blue).

$z_S = 1$, but these terms are probably too small to be detected in real data.

In Fig. 8 (top panel) we show the total $C_\ell(z_S)$'s smeared with a 10% window function. Comparing it with Fig. 2, we mainly notice that the power is reduced significantly, by nearly 1.5 orders of magnitude. Furthermore, at $z_S = 0.1$, the baryon acoustic oscillations are clearly visible. In the presence of a window, different terms can dominate at different redshift and for different values of ℓ. In the bottom panel of Fig. 8, we depict the ratio between the new contributions and the total angular power spectrum. Neglecting the new contributions induces an error of a few percent already at redshift 1, and this error increases to roughly 50% at redshift 3. Note that this ratio depends

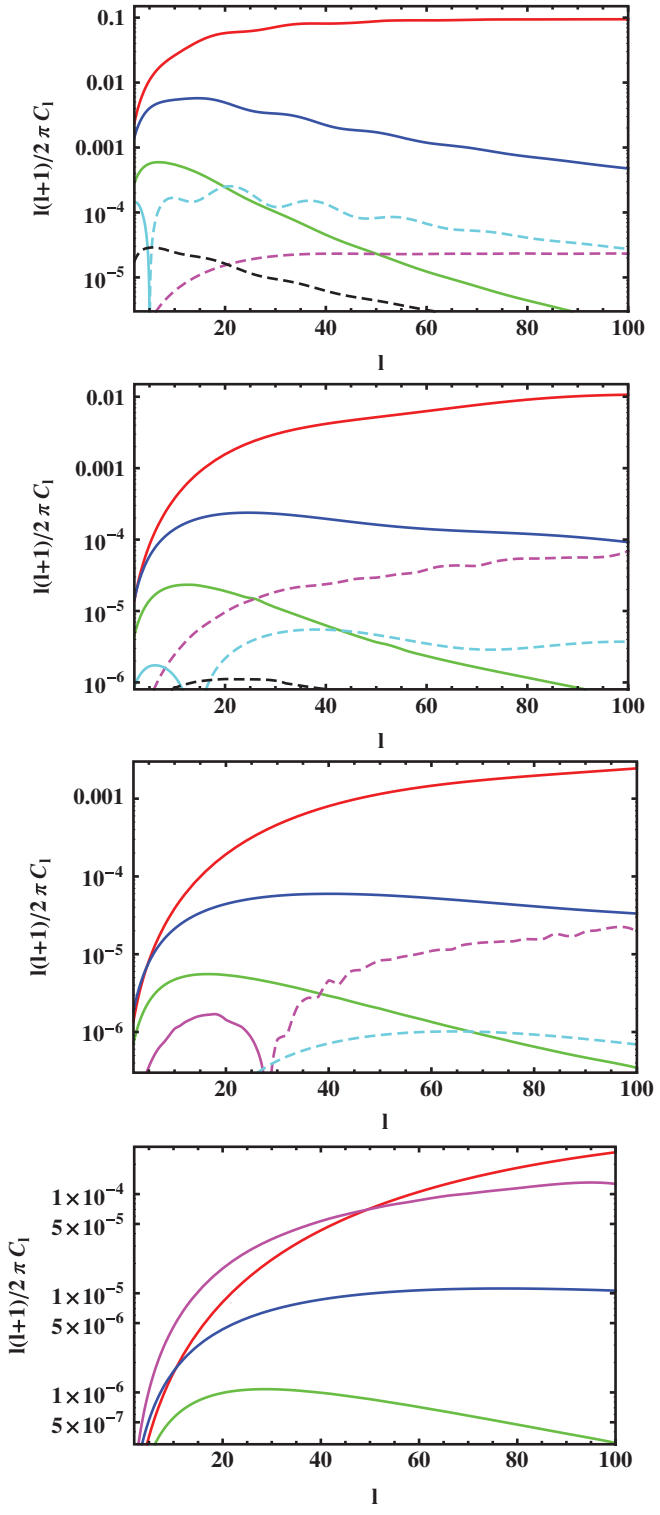

FIG. 7 (color). The effect of a window function with width $\Delta z_S = 0.1 z_S$ on the power spectrum $C_\ell(z_S)$ for redshifts (from top to bottom) $z_S = 0.1$, 0.5, 1, and 3. The different curves are as follows: density (red line), redshift-space distortion (green line), the correlation of density with redshift-space distortion (blue line), lensing (magenta line), Doppler (cyan line), and gravitational potential (black line); see Table I. Solid lines denote positive contributions whereas dashed lines denote negative contributions.

strongly on the width of the window function, and that a wider window would lead to a larger error.

In Fig. 9 (top panel) we plot the different terms as a function of redshift, for a fixed value of $\ell = 20$. Contrary to Fig. 4, where the lensing term always remains subdominant with respect to the density and redshift-space distortion term, we see in Fig. 9 that for $z_S > 2.4$ the lensing term dominates over the standard contribution. The redshift at which this dominance takes place depends of course on the chosen window function: for larger Δz_S, the lensing term starts to dominate at smaller redshift. In the bottom panel of Fig. 9 we show the ratio between the new contributions and the total angular power spectrum as a function of redshift for $\ell = 20$. From this figure we understand why in Fig. 8 (bottom panel), the ratio at $z_S = 1$ is not significantly larger than at $z_S = 0.5$. The lensing contribution changes sign around $z_S = 0.9$, and consequently, it is still small at $z_S = 1$. At a redshift of $z_S = 1.5$, however, the error induced by neglecting the new terms is already of the order of 10%.

In Fig. 10 we show correlations between different redshifts bins (with a 10% window function), for a fixed value

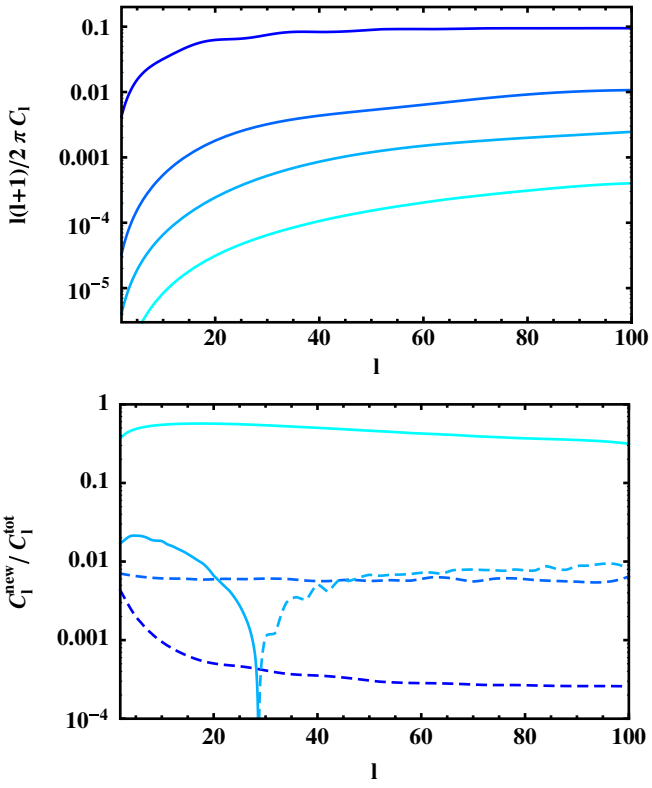

FIG. 8 (color online). Top panel: The total power spectrum at redshifts (from top to bottom) $z_S = 0.1$, $z_S = 0.5$, $z_S = 1$, and $z_S = 3$ smeared by a window function with width $\Delta z_S = 0.1 z_S$. Bottom panel: The ratio between the new contributions (lensing + potential) and the total angular power spectrum at (from top to bottom) $z_S = 3$, $z_S = 1$, $z_S = 0.5$, and $z_S = 0.1$. Solid lines denote positive contributions whereas dashed lines denote negative contributions.

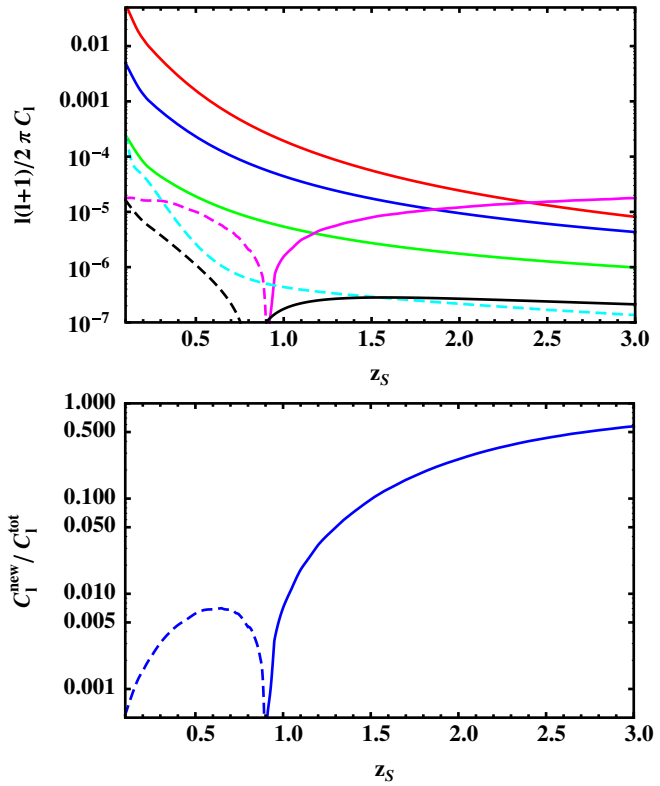

FIG. 9 (color online). The various terms as a function of z_S for a fixed value of $\ell = 20$ and smeared by a window function with width $\Delta z_S = 0.1 z_S$: density (red line), redshift-space distortion (green line), the correlation of density with redshift-space distortion (blue line), lensing (magenta line), Doppler (cyan line), and potential (black line); see Table I. Here the correlations between the lensing and Doppler and the lensing and potential are not negligible at large z_S, and they are included in the Doppler (cyan line), respectively, potential (black line) curves. Solid lines denote positive contributions; dashed lines denote negative contributions. Bottom panel: The ratio between the new contributions (lensing + potential) and the total angular power spectrum, smeared by a window function with width $\Delta z_S = 0.1 z_S$, plotted as a function of z_S for a fixed value of $\ell = 20$.

of $\ell = 20$. As in Fig. 5 we see that the lensing term becomes dominant when the redshift separation between the bins increases. At large redshift, $z_S = 3$, the lensing term is always dominant. The individual behavior of each contribution is, however, quite different from Fig. 5 which is due to the smearing introduced by the window function. Note that comparing the second panel in Fig. 10 with the results in [20], we see that the redshift separation between their four different bins (their Fig. 13) is too small for the lensing contribution to be relevant. However, a similar measurement with one of the bins situated around $z_S = 0.7$ would already allow us to detect the lensing contribution.

Finally, we plot in Fig. 11 the angular power spectrum integrated from the observer until a maximum redshift $z_{\max}$. This corresponds to the situation where the redshifts

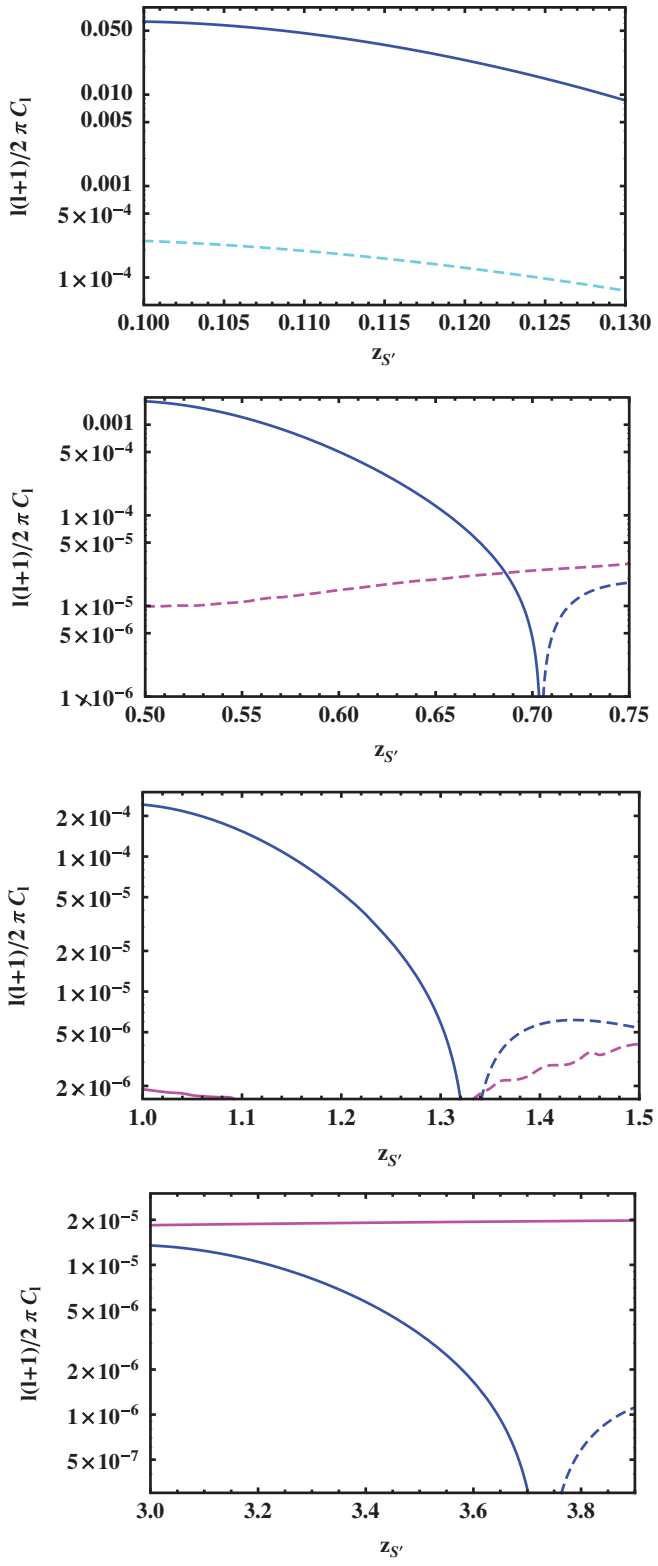

FIG. 10 (color). Cross correlations between different redshift bins $C_\ell(z_S, z_{S'})$ at $\ell = 20$ with a 10% window function and plotted as a function of $z_{S'}$. From top to bottom $z_S = 0.1$, 0.5, 1, and 3. The standard term, i.e. $C_\ell^{DD} + C_\ell^{zz} + 2C_\ell^{Dz}$ (blue line), lensing (magenta line), Doppler (cyan line), and potential (black line) are shown; see Table I. Solid lines denote positive contributions whereas dashed lines denote negative contributions.

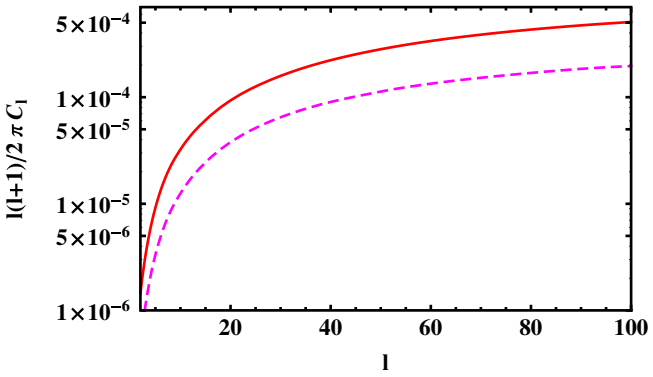

FIG. 11 (color online). Integrated power spectrum with a flat distribution between $z_{\min} = 0.1$ and $z_{\max} = 2$ with Gaussian tails at both ends. The density term is plotted in red and the lensing term in magenta. Note that the lensing term is completely dominated by its anticorrelation with the density and hence is negative.

of individual galaxies are unknown but obey a given redshift distribution. Consequently, only the integrated spectrum can be measured. We assume a flat distribution of galaxies between $z_{\min} = 0.1$ and $z_{\max} = 2$ with Gaussian tails at both ends. In Fig. 11 we see that the only relevant contributions are the density and the lensing, more precisely the cross correlation between the lensing and the density which is negative. The redshift-space distortion contribution is, as expected, completely negligible when the galaxy redshifts are unknown. The lensing contribution, however, is very relevant; it reduces the result by roughly 40% of the contribution from the density alone.

IV. CONCLUSIONS

In this paper we have derived expressions for the transversal and radial galaxy power spectra, $C_\ell(z_S)$ and $C_\ell(z_S, z_{S'})$, taking into account not only redshift-space distortions, which have also been studied e.g. in [20], but also all other relativistic effects to first order in perturbation theory. Within our accuracy we are in reasonable agreement with the simulated results of Ref. [20] (their Fig. 4) which analyzes the Sloan Digital Sky Survey data, taking into account redshift-space distortion but not the other terms, e.g. the lensing, appearing in our formula (31). They also take into account nonlinearities in the matter power spectrum by using HALOFIT [17]. This enhances their results with respect to ours.

We have seen that by measuring $C_\ell(z_S, z_{S'})$ for different redshift differences and different ℓ's, we can measure different combinations of terms which depend on cosmological parameters in a variety of ways. Otherwise, one may measure the C_ℓ's smeared over a given redshift bin, Δz_S,

$$C_\ell(z_S, \Delta z_S) = \int dz dz' W(z, z') C_\ell(z, z'),$$

where W is a window function centered at z_S with width Δz_S. Without smearing, the density contribution and the redshift-space distortion always dominate. When smearing is included these terms are reduced and the lensing term can dominate.

The method outlined in this paper represents a very flexible new path to estimate cosmological parameters and to test the consistency of the concordance model of cosmology. Of course, to do this we must master possible degeneracies, not only with biasing but also evolutionary effects which have not been discussed in this work and which may become relevant at redshifts larger than 1; see [21] for a discussion. A detailed parameter estimation forecast e.g. for Euclid is left as a future project.

ACKNOWLEDGMENTS

We thank Anthony Lewis and Anthony Challinor who were accidentally working on a very similar project [21]. We compared our results with theirs, and although the derivation is different, the analytical results completely agree. Anthony Lewis also shared their numerical results with us. This comparison helped us considerably, and we also agree on the numerical part. We acknowledge useful discussions with Francis Bernardeau, Chiara Caprini, Chris Clarkson, Martin Kunz, Roy Maartens, and Francesco Montanari. We thank the referee for useful suggestions. R. D. is supported by the Swiss National Science Foundation. C. B. is supported by a Herchel Smith Postdoctoral Fellowship and by King's College Cambridge.

APPENDIX A: SOME DETAILS OF THE DERIVATIONS FOR $\Delta(\mathbf{n}, z)$

We consider a perturbed Friedmann metric,

$$ds^2 = a^2(t)(-(1 + 2A)dt^2 - 2B_i dt dx^i + [(1 + 2H_L)\delta_{ij} + 2H_{Tij} + 2H_{ij}]dx^i dx^j). \quad \text{(A1)}$$

Here H_{ij} is the transverse traceless gravitational wave term and A, B_i, H_L, and H_{Tij} are scalar degrees of freedom, two of which can be removed by gauge transformations. In Fourier space $B_i = -\hat{k}_i B$ and $H_{Tij} = (\hat{k}_i \hat{k}_j - \delta_{ij}/3)H_T$. Often one uses longitudinal (or Newtonian) gauge with $B = H_T = 0$, but we shall not use longitudinal gauge here. This is useful if we want to determine whether a given expression is gauge invariant. In a generic gauge, the gauge-invariant Bardeen potentials Φ and Ψ are given by [22]

$$\Psi \equiv A + \frac{\mathcal{H}}{k} B + \frac{1}{k}\dot{B} - \frac{\mathcal{H}}{k^2}\dot{H}_T - \frac{1}{k^2}\ddot{H}_T, \quad \text{(A2)}$$

$$\Phi \equiv -H_L - \frac{1}{3}H_T + \frac{\mathcal{H}}{k^2}\dot{H}_T - \frac{\mathcal{H}}{k} B. \quad \text{(A3)}$$

In longitudinal gauge they reduce to $A = \Psi$, $H_L = -\Phi$.

From this we easily obtain the following expressions for the redshift perturbation [1,11],

$$\frac{\delta z}{1+z} = -\Big[\Big(H_L + \frac{1}{3}H_T + \mathbf{n}\cdot\mathbf{V} + \Phi + \Psi\Big)(\mathbf{n}, z) + \int_0^{r_S}(\dot\Phi + \dot\Psi + \dot H_{ij}n^i n^j)d\lambda\Big] \tag{A4}$$

which leads to the density fluctuation in redshift space given in Eq. (8). To determine the volume perturbation we have to compute the derivative,

$$\frac{d\delta r}{d\lambda} = -(\Phi+\Psi) + \frac{1}{k}\frac{dB}{d\lambda} + \frac{1}{k^2}\Big(\frac{d^2H_T}{d\lambda^2} - 2\frac{d\dot H_T}{d\lambda}\Big) - H_{ij}n^i n^j. \tag{A5}$$

Here we made use of the fact that the Fourier transforms of B_i and H_{Tij} are, respectively,

$$B_i(\mathbf{k}, t) = -\frac{1}{k}\partial_i B, \tag{A6}$$

$$H_{Tij}(\mathbf{k}, t) = \frac{1}{k^2}\partial_i\partial_j H_T + \frac{1}{3}\delta_{ij}H_T. \tag{A7}$$

Using $\frac{dX}{d\lambda} = \dot X + n^i\partial_i X = \dot X - \partial_r X$, we then obtain

$$\begin{aligned} B_i n^i &= -\frac{1}{k}\frac{dB}{d\lambda} + \frac{1}{k}\dot B, \qquad B_i e^i_\theta = -\tfrac{1}{kr}\partial_\theta B,\\ H_{Tij}n^i n^j &= \frac{1}{k^2}\Big(\frac{d^2H_T}{d\lambda^2} - 2\frac{d\dot H_T}{d\lambda} + \ddot H_T\Big) + \frac{1}{3}H_T\\ &= \frac{1}{k^2}\partial_r^2 H_T + \frac{1}{3}H_T,\\ H_{Tij}e^i_\theta n^j &= \frac{\partial_\theta}{k^2 r}\Big(\frac{dH_T}{d\lambda} - \dot H_T\Big) + \frac{\partial_\theta}{(kr)^2}H_T. \end{aligned}$$

Similar relations hold for e^i_φ. The angular volume perturbation is

$$\begin{aligned} \Big(\frac{\delta v}{v}\Big)_\Omega &\equiv (\cot\theta + \partial_\theta)\delta\theta + \partial_\varphi\delta\varphi\\ &= \frac{-1}{r_S}\int_0^{r_S} d\lambda\frac{(r_S - r)}{r}\Delta_\Omega(\Phi+\Psi) - \frac{\Delta_\Omega H_T(t_S)}{(kr_S)^2}\\ &\quad - \int_0^{r_S} d\lambda\Big[\frac{(r_S-r)}{r_S r}\Delta_\Omega(H_{ij}n^i n^j) + \frac{2}{r}\Big((\cot\theta + \partial_\theta)\\ &\quad \times(H_{ij}n^i e^j_\theta) + \frac{1}{\sin\theta}\partial_\varphi(H_{ij}n^i e^j_\varphi)\Big)\Big]. \end{aligned} \tag{A8}$$

Here Δ_Ω denotes the angular part of the Laplacian. The second integral in Eq. (A8) is the contribution from gravitational waves which we shall not discuss further in this work.

Putting it all together in Eq. (17), using also Eq. (29) for the derivative of the perturbed redshift, we obtain the volume perturbation at fixed conformal time t or fixed background redshift $\bar z$. However, we need to evaluate the volume fluctuation at a fixed, *observed* redshift which is related to the latter by

$$\begin{aligned} \frac{\delta v}{\bar v}\Big|_z &= \frac{\partial_z\bar v\delta z + \delta v(\bar z)}{\bar v}\\ &= \frac{\delta v(\bar z)}{\bar v} + \Big(\frac{2}{r_S\mathcal{H}} - 4 + \frac{\dot{\mathcal{H}}}{\mathcal{H}^2}\Big)\frac{\delta z}{1+z}\\ &= 3H_L - \mathbf{v}\cdot\mathbf{n} + \Big(\frac{\delta v}{v}\Big)_\Omega + \frac{2\delta r}{r_S} - \frac{d\delta r}{d\lambda}\\ &\quad + \frac{1}{\mathcal{H}(1+z)}\frac{d\delta z}{d\lambda} + \Big(\frac{2}{r_S\mathcal{H}} - 4 + \frac{\dot{\mathcal{H}}}{\mathcal{H}^2}\Big)\frac{\delta z}{1+z}. \end{aligned} \tag{A9}$$

To simplify the expressions we combine the terms $(d^2H_T/d\lambda^2 - 2d\dot H_T/d\lambda)/k^2$ of $\frac{d\delta r}{d\lambda}$ and $2/(k^2 r_S)dH_T/d\lambda$ of $2\delta r/r$ with $\Delta_\Omega H_T/(kr_S)^2$ of the angular volume perturbation to

$$\begin{aligned} &-\frac{1}{k^2}\Big(\frac{d^2H_T}{d\lambda^2} - 2\frac{d\dot H_T}{d\lambda} - \frac{2}{r_S}\frac{dH_T}{d\lambda} + \frac{\Delta_\Omega H_T}{r_S^2}\Big)\\ &= -\frac{1}{k^2}(\Delta H_T - \ddot H_T - \frac{2}{r_S}\dot H_T) = H_T + \frac{1}{k^2}\Big(\ddot H_T + \frac{2}{r_S}\dot H_T\Big). \end{aligned}$$

We also use the gauge-invariant velocity potential [1,11]

$$V \equiv \mathrm{v} - \frac{1}{k}\dot H_T \tag{A10}$$

so that

$$\mathbf{v}\cdot\mathbf{n} = -\frac{1}{k}n^i\partial_i v = \mathbf{V}\cdot\mathbf{n} - \frac{1}{k^2}n^i\partial_i\dot H_T, \tag{A11}$$

and the derivative of Φ along the light ray,

$$\frac{1}{\mathcal{H}}\frac{d\Phi}{d\lambda} = -\frac{1}{\mathcal{H}}\frac{d}{d\lambda}\Big(H_L + \frac{H_T}{3}\Big) + \frac{1}{k^2}\Big(\frac{d\dot H_T}{d\lambda} + \frac{\dot{\mathcal{H}}}{\mathcal{H}}\dot H_T\Big) - \frac{1}{k}\Big(\frac{dB}{d\lambda} + \frac{\dot{\mathcal{H}}}{\mathcal{H}}B\Big). \tag{A12}$$

With the help of these identities, the volume density perturbation reduces to the gauge-invariant expression (30), where the gravitational wave contribution is omitted for simplicity.

APPENDIX B: THE CONTRIBUTIONS TO THE ANGULAR POWER SPECTRUM

In this appendix we express certain contributions to the total $C_\ell's$ which are of particular interest for the discussion given in the text. We use the transfer functions for the concordance model given in Eqs. (45)–(48).

Density fluctuation: Let us first consider the density term. The term of T_D in (46) proportional to k^2T_Ψ largely dominates the integral. Its contribution is

$$C_\ell^{DD}(z_S) = \frac{2A}{\pi}\left(\frac{9}{10}\right)^2 \frac{4a_S^2}{9\Omega_m^2}\left(\frac{D_1(a_S)}{a_S}\right)^2 \times \int \frac{dk}{k}\left(\frac{k}{\mathcal{H}_0}\right)^4 T^2(k) j_\ell^2(kr_S). \quad \text{(B1)}$$

This integral only converges since $T(k)$ decays like $1/k^2$ for $k > k_{\rm eq}$, where $k_{\rm eq}$ is the (comoving) horizon scale at equal matter and radiation; see e.g. [1]. This integral is always dominated by the fluctuations on this scale, even at low $\ell \ll \ell_{\rm eq}(z_S) \simeq \pi k_{\rm eq} r(z_S)$.

Redshift-space distortion: The term $T_V^2(k)(j_\ell''(kr_S))^2$ coming from $\partial_r(\mathbf{V}\cdot\mathbf{n})$ is the redshift-space distortion. Since it is multiplied by $k/\mathcal{H}$ its dominant contribution behaves like the density term and is of the same order,

$$C_\ell^{zz}(z_S) = \frac{2A}{\pi}\left(\frac{9}{10}\right)^2 \frac{4a_S^2}{9\Omega_m^2}\left[\frac{D_1(a_S)}{a_S} + a_S\frac{d}{da_S}\left(\frac{D_1(a_S)}{a_S}\right)\right]^2 \times \int \frac{dk}{k}\left(\frac{k}{\mathcal{H}_0}\right)^4 T^2(k) j_\ell''^2(kr_S). \quad \text{(B2)}$$

Cross-term density-redshift-space distortion: Also this term is of the same order as the previous two and even dominates at low ℓ.

$$C_\ell^{Dz}(z_S) = -\frac{2A}{\pi}\left(\frac{9}{10}\right)^2 \frac{4a_S^2}{9\Omega_m^2}\left[\frac{D_1(a_S)}{a_S} + a_S\frac{d}{da_S}\left(\frac{D_1(a_S)}{a_S}\right)\right] \times \frac{D_1(a_S)}{a_S}\int \frac{dk}{k}\left(\frac{k}{\mathcal{H}_0}\right)^4 T^2(k) j_\ell(kr_S) j_\ell''(kr_S). \quad \text{(B3)}$$

Lensing: The lensing contribution is, in principle, also of the same order. But since it probes the power spectrum truly at $k \simeq \ell/r(z_S)$, it is largely subdominant at low ℓ if compared to the previous contributions.

$$\begin{aligned} C_\ell^{LL}(z_S) &= \frac{8A}{\pi}\left(\frac{9}{10}\right)^2 \ell^2(\ell+1)^2 \frac{1}{r_S^2}\int \frac{dk}{k} T^2(k) \\ &\quad \times \left[\int_0^{r_S} d\lambda \frac{r_S - r}{r}\frac{D_1(a)}{a} j_\ell(kr)\right]^2 \\ &= 4A\frac{\ell^2(\ell+1)^2}{(\ell+1/2)^3}\left(\frac{9}{10}\right)^2 \int_0^{r_S}\frac{dr}{r}\frac{(r_S - r)^2}{r_S^2} \\ &\quad \times \left(\frac{D_1(r)}{a(r)}\right)^2 T^2\left(\frac{\ell+1/2}{r}\right). \end{aligned} \quad \text{(B4)}$$

In the last equality we have used Limber's approximation [18],

$$\int_0^{y_S} dy f(y) J_\nu(y) = f(\nu)\theta(y_S - \nu) + O\left(\frac{1}{\nu^2}\right). \quad \text{(B5)}$$

Cross-term density lensing:

$$\begin{aligned} C_\ell^{LD}(z_S) &= -\frac{8A}{3\pi}\left(\frac{9}{10}\right)^2 \frac{\ell(\ell+1)}{\Omega_m r_S}\int \frac{dk}{k} T^2(k)\left(\frac{k}{\mathcal{H}_0}\right)^2 \\ &\quad \times \frac{1}{1+z_S}\frac{D_1(a_S)}{a_S} j_\ell(kr_S)\int_0^{r_S} d\lambda \frac{r_S - r}{r} \\ &\quad \times \frac{D_1(a)}{a} j_\ell(kr) \\ &= -\frac{8A}{3\pi}\sqrt{\frac{\pi}{2}}\left(\frac{9}{10}\right)^2 \frac{\ell(\ell+1)\sqrt{\nu}}{\Omega_m(1+z_S)}\frac{D_1(a_S)}{a_S} \\ &\quad \times \int_0^{r_S}\frac{dr}{r^3} T^2\left(\frac{\ell+1/2}{r}\right)\frac{r_S - r}{r_S}\frac{D_1(r)}{a(r)} j_\ell\left(\frac{\nu r_S}{r}\right). \end{aligned} \quad \text{(B6)}$$

The other terms are as follows.

Velocity:

$$C_\ell^{VV}(z_S) = \frac{2A}{\pi}\left(\frac{9}{10}\right)^2 \frac{4a_S^2}{9\Omega_m^2}\left[\frac{D_1(a_S)}{a_S} + a_S\frac{d}{da_S}\left(\frac{D_1(a_S)}{a_S}\right)\right]^2 \times \left(\frac{\mathcal{H}_S}{\mathcal{H}_0}\right)^2\left(\frac{\dot{\mathcal{H}}_S}{\mathcal{H}_S^2} + \frac{2}{r_S\mathcal{H}_S}\right)^2 \cdot \int \frac{dk}{k}\left(\frac{k}{\mathcal{H}_0}\right)^2 \times T^2(k) j_\ell'^2(kr_S). \quad \text{(B7)}$$

Cross-term redshift-space distortion velocity:

$$C_\ell^{zV}(z_S) = \frac{2A}{\pi}\left(\frac{9}{10}\right)^2 \frac{4a_S^2}{9\Omega_m^2}\left[\frac{D_1(a_S)}{a_S} + a_S\frac{d}{da_S}\left(\frac{D_1(a_S)}{a_S}\right)\right]^2 \times \frac{\mathcal{H}_S}{\mathcal{H}_0}\left(\frac{\dot{\mathcal{H}}_S}{\mathcal{H}_S^2} + \frac{2}{r_S\mathcal{H}_S}\right)\cdot \int \frac{dk}{k}\left(\frac{k}{\mathcal{H}_0}\right)^3 \times T^2(k) j_\ell'(kr_S) j_\ell''(kr_S). \quad \text{(B8)}$$

Cross-term density velocity:

$$C_\ell^{DV}(z_S) = -\frac{2A}{\pi}\left(\frac{9}{10}\right)^2 \frac{4a_S^2}{9\Omega_m^2}\frac{D_1(a_S)}{a_S}\left[\frac{D_1(a_S)}{a_S} + a_S\frac{d}{da_S} \times \left(\frac{D_1(a_S)}{a_S}\right)\right]\frac{\mathcal{H}_S}{\mathcal{H}_0}\left(\frac{\dot{\mathcal{H}}_S}{\mathcal{H}_S^2} + \frac{2}{r_S\mathcal{H}_S}\right)\cdot \int \frac{dk}{k}\left(\frac{k}{\mathcal{H}_0}\right)^3 \times T^2(k) j_\ell(kr_S) j_\ell'(kr_S). \quad \text{(B9)}$$

In the regimes investigated in this work the gravitational potential terms are always subdominant and we do not write them down explicitly.

[1] R. Durrer, *The Cosmic Microwave Background* (Cambridge University Press, Cambridge, England, 2008).
[2] H. Tadros *et al.*, Mon. Not. R. Astron. Soc. **305**, 527 (1999); L. Samushia, W. J. Percival, and A. Raccanelli, arXiv:1102.1014.
[3] C. Alcock and B. Pacinski, Nature (London) **281**, 358 (1979).
[4] J. Yoo, M. Zaldarriaga, and L. Hernquist, Phys. Rev. D **81**, 123006 (2010); J. Yoo, Phys. Rev. D **82**, 083508 (2010).
[5] BOSS, http://www.sdss3.org/.
[6] DES, http://www.darkenergysurvey.org/.
[7] Pan-STARRS, http://pan-starrs.ifa.hawaii.edu/public/.
[8] Euclid, http://sci.esa.int/euclid.
[9] K. Abazajian *et al.*, Astrophys. J. Suppl. Ser. **182**, 543 (2009); B. Reid *et al.*, Mon. Not. R. Astron. Soc. **404**, L60 (2010).
[10] This is not what is done in practice, where the observed ''point process'' i.e. the observed distribution of galaxies is compared to a random one with the same redshift distribution (but usually many more galaxies to reduce scatter [9]).
[11] R. Durrer, Fundam. Cosm. Phys. **15**, 209 (1994).
[12] C. Bonvin, Phys. Rev. D **78**, 123530 (2008).
[13] F. Bernardeau, C. Bonvin, and F. Vernizzi, Phys. Rev. D **81**, 083002 (2010).
[14] Abramowitz and I. Stegun, *Handbook of Mathematical Functions* (Dover Publications, New York, 1970), 9th ed.
[15] S. Dodelson, *Modern Cosmology* (Academic Press, New York, 2003).
[16] T. Hui-Ching Lu, K. Ananda, C. Clarkson, and R Maartens, J. Cosmol. Astropart. Phys. 02 (2009) 023.
[17] A. Lewis, A. Challinor, and A. Lasenby, Astrophys. J. **538**, 473 (2000).
[18] M. LoVerde and N. Afshordi, Phys. Rev. D **78**, 123506 (2008).
[19] N. Kaiser, Mon. Not. R. Astron. Soc. **227**, 1 (1987).
[20] S. A. Thomas, F. B. Abdalla, and O. Lahav, Mon. Not. R. Astron. Soc. **412**, 1669 (2011).
[21] A. Challinor and A. Lewis, arXiv:1105.5292.
[22] J. Bardeen, Phys. Rev. D **22**, 1882 (1980).